# USP wave basin: active wave absorption and generation algorithms

**Mario L. Carneiro[1], Pedro C. de Mello[1], Felipe Labate[1], André A. M. Araujo[1], Alexandre N. Simos[2] and Eduardo A. Tannuri[1]**

1 Dept. Mechatronics Engineering, USP
eduat@usp.br
2 Dept. Naval Architecture and Ocean Engineering, USP
Numerical Offshore Tank - TPN-USP

## Abstract

This paper presents the analysis of wave absorption and generation algorithms that were latter applied in the new wave basin constructed at the University of São Paulo (USP), as part of the Numerical Offshore Tank (TPN) Laboratory. These algorithms calculate the motions of the wave makers both to generate and absorb the required wave field by taking into account the layout of the flaps and the limits of wave generation. In order to study different aspects of the implementation, the performance of a prototype device composed of 4 flaps was evaluated in a 2D wave flume, prior to the assembly of the complete system at the TPN wave basin. The generation algorithms are based on the summation of wave components (frequencies and directions) obtained from the required directional wave spectrum. The transfer function that relates the flap motion to the generated wave is considered. Absorption tests were conducted using two different algorithms: a frequency domain method based on Maeda et al. (2004), in which the controlled variable is the motor velocity, and the time domain algorithm proposed by Schäffer (2001). The latter is based on a digital filter and the position of the flap is the variable to be controlled. Both algorithms require hydrodynamic feedback based on the measurement of the surface elevation at each flap. The first algorithm needs an extensive test procedure to calibrate its control parameters, while the second one, after optimizing the digital filter, should be ready to use. Both algorithms presented similar results with reflection coefficients smaller than 10.7% for regular waves with frequencies ranging from 0.5 to 1.5 Hz.

## Keywords

Wave Basin, Wave Absorption, Segmented Wave Maker, Reflection Coefficient, Digital Filter.

## 1 Introduction

This paper presents a detailed description of the algorithms development for the new active absorption wave basin built at the University of São Paulo (USP), a part of the Numerical Offshore Tank (TPN) Laboratory. The tank is intended to be used as a calibration tool for the numerical models employed for the dynamic simulation of offshore structures and vessels. Furthermore, it may be used as an efficient basin for testing the station keeping performance and motions of floating units in several kinds of wave fields. One of the main goals pursued during its design was that the facility should have a simple and flexible operation and easy maintenance. In order to achieve this feature, the wave basin was conceived to be small. Active wave absorption was then considered as a means for reducing wave reflections.

The new facility is under development at the University of São Paulo since 2006. It consists of a 14m x 14m rectangular wave tank with a depth of 4m and a wave generation-absorption system based on 148 flap-type wave makers. To develop the active absorption system, each wave maker has an ultrasonic sensor that measures the instantaneous water level in its face. A high level control system interface is present to allow the development of the control algorithms.

The system described by Salter (1981) was the first operational active absorption system in a multidirectional wave basin. Active wave absorption has also been used in two newly opened facilities: The Amoeba (Advanced Multiple Organized Experimental Basin) wave tank in Osaka (Naito et al. (1996) and Naito (2006)) is a prototype tank of variable geometry. Wave making is based on a system of plungers and the wave absorption control is performed by monitoring the vertical velocity and the force on each wave maker. A much larger facility was opened in 2002 at the National Maritime Research Institute (NMRI) in Tokyo. The Deep--Sea basin (Maeda et al (2004)) consists of a circular wave tank with a diameter of 16m, equipped with a set of 128 flap-type wave makers along its circumference. The methodology for absorption control is different from the one employed at the Amoeba basin: wave-probes mounted on each flap measure the wave elevation continuously and, by comparing it with predicted values, provide the data necessary to correct the input signal for flap motion in order to absorb the reflected waves.

*Submitted to MS&OT on Sep 09 2010. Revised version submitted on Nov 16 2010. Accepted on Dec 10 2010. Editor:* ***Marcelo A. S. Neves****.*

This paper intends to describe the analysis, validation and preliminary calibration of the generation and active absorption algorithms. This work was executed in a 2D wave flume, that was the workbench used for developing all the algorithms later implemented in the TPN wave basin. Wave generation is based on the time realization of frequency domain transfer functions for each flap, considering linear superposition of the individual responses. Preliminary tests conducted with a small scale device were used to evaluate the performance of the absorption algorithms, one of the main issues of the wave tank. Two different algorithms were tested. The first one is the frequency domain method based on Maeda et al. (2004) and the second is the time domain algorithm proposed by Schäffer (2001). Tests indicated the advantages of the second method that was then in fact implemented in the wave tank. The commissioning and preliminary operation of the TPN wave basin is described by de Mello et al. (2009).

## 2 Wave generation algorithms

The wave generation theory using flap-type wave makers is well addressed in the specialized literature. In the linear theory context, multi-directional waves can be generated by the summation of many wave components with different frequencies and directions, as described by Nohara et al. (1996). The summation in frequency can be made according to a prescribed power spectrum ($S(w)$), while the summation in direction follows a energy spreading function ($D(\theta)$). The final result is a short-crested wave field, as indicated in eqs. 2.1 and 2.2. When the summation is made only in frequency, the result is a long-crested sea ($D(\theta)$ is zero for every direction other than the prescribed wave direction). Regular waves are obtained by considering only one amplitude and one frequency.

$$X_i(t)=\sum_{n=1}^{N}\sum_{m=1}^{M}\frac{a_{nm}}{F_n}\cdot cos(2\pi f_n t - ik_n \ell sin\theta_m + \varepsilon_{nm})\cdot cos\theta_m \quad (2.1)$$

where $a_{nm}$ is the wave amplitude of the component of frequency $n$, and direction $m$, given by:

$$a_{nm} = (2\cdot S(w_n)\cdot D(\theta_m)\cdot \Delta w\cdot \Delta\theta)^{1/2} \quad (2.2)$$

and:

$X_i$ : i-th wave maker stroke (position)
$N$ : Number of frequency components
$M$ : Number of directional components
$I$ : Number of wave makers
$F_n$ : n-th frequency 2D flap transfer function for the flap at driven height
$f_n$ : n-th wave frequency
$\ell$ : Wave maker width
$\theta_m$ : m-th wave direction
$k_n$ : n-th wave number
$\varepsilon_{nm}$ : Random phase in the interval [0...2$\pi$]
$S(w_n)$ : Power spectrum (m²s)
$D(\theta_m)$ : Energy spread function with $\int_0^{2\pi} D(\theta)\,d\theta = 1$

The transfer function Fn that relates the flap stroke to the wave amplitude is discussed in the next section.

Considering the geometry of the wave basin, the required number of active flaps depends on the desired ranges of wave frequencies and directions to be generated (de Mello et al, 2009). The TPN wave basin is composed of 148 active flaps (two of its sides are equipped with 39 flaps and the other two have 35 active flaps each). Therefore, the generation of oblique waves by two adjacent sides requires the activation of 74 flaps. In the same way, when directional spreading is considered, the number of directions increases and more flaps must be activated to generate the desired wave. For example, for delivering a short-crested wave with 0º mean direction and energy spreading from -180º to 180º, three sides of the wave basin must be used (109 flaps).

The wave generation algorithm was implemented using MATLAB®. Concerning the computation effort required for processing the generation data, the regular wave takes short time to be executed, while the long-crested wave has an intermediate computational cost and the short-crested wave is quite demanding. The calculation of each flap motion is done by a pre-processor and the time series are generated and loaded by the wave generator real-time control software. Table 1 provides a comparative example of the computational cost required to compute the time series for different wave fields. All cases consider wave generation for a period of 120 seconds, sample rate of 83Hz, two mean directions, 540 frequency components and 36 direction components when applicable.

**Table 1** Example of the computational cost required to calculate the time series

| Wave type | Angle | Sample rate (Hz) | N | M | I | Series time (s) | Processing time (s) |
|---|---|---|---|---|---|---|---|
| Regular | 0° | 83 | 1 | - | 39 | 120 | 2.54 |
| | 45° | 83 | 1 | - | 74 | 120 | 2.54 |
| Irregular long-crested | 0° | 83 | 540 | - | 39 | 120 | 38 |
| | 45° | 83 | 540 | - | 74 | 120 | 68 |
| Irregular short-crested | 0° | 83 | 540 | 36 | 109 | 120 | 540 |
| | 45° | 83 | 540 | 36 | 74 | 120 | 566 |

## 3 Wave generation transfer function

The wave generation transfer function relates the progressive wave amplitude ($A_I$) generated in the tank with the amplitude of the sinusoidal motion ($X_0$) of each flap, for different wave frequencies. It is discussed, for example, in Dean and Dalrymple (1984) or Schäffer (1996). At a distance far enough from the wave generator, the transfer function can be written as:

$$\frac{A_I}{X_0} = ie_0 = \frac{i}{cos\,\theta}c_0 \quad (3.1)$$

where i is the imaginary number and represents the 90o phase shift between the wave and the flap movement, $\theta$ is the wave propagation direction. For a flap type wave generator, $c_0$ can be written as:

$$c_0 = \left(\frac{4\,sinh(k_p h)}{k_p h_2}\right)\left(\frac{k_p(h-h_1)\,sinh(k_p h) - cosh(k_p h) + cosh(k_p h_1)}{sinh(2k_p h) + 2k_p h}\right) \quad (3.2)$$

where $k_p$ is the wave number of the progressive wave, $h$ is the depth of the tank, $h_1$ is the vertical distance from the tank bottom to the flap pivot point and $h_2$ is the flap total height.

Closer to the wave maker, localized effects (also known as evanescent wave modes) are observed:

$$\frac{A_0}{X_0} = i\left(e_0 + \sum_{j=1}^{\infty} e_j\right) \tag{3.3}$$

where $A_0$ is the complex amplitude of the wave level measured in front of the flap and $e_j$ is the transfer function of the $j$-th evanescent wave mode, which, for a flap type wave generator, is given by:

$$e_j = \frac{k_j}{k_{xj}} c_j = \frac{k_j}{k_{xj}} \left(\frac{-4\,sin(k_j h)}{k_j h_2}\right) \left(\frac{k_j(h_1-h)\,sin(k_j h) - cos(k_j h) + cos(k_j h_1)}{sin(2k_j h) + 2k_j h}\right) \tag{3.4}$$

in which $k_j$ is the wave number of the evanescent mode j and $k_{xj}$ is its x-component.

An example comparing the progressive wave transfer function $A_1 / X_0$ (equation 3.1) and the full wave generation transfer function $A_0/X_0$ that includes progressive and evanescent modes (equation 3.3) is shown in Figure 1:

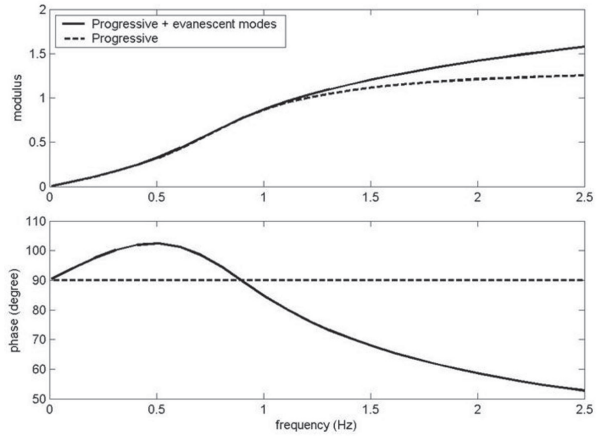


Fig. 1 Wave generation transfer functions

## 4 Absorption algorithm A

The first absorption algorithm tested is based on the one proposed by Maeda (2004). This algorithm uses hydrodynamic feedback based on the measurement of wave elevation at each flap and flap velocity as a reference for the control.

Neglecting the evanescent wave modes, it can be shown that there is no phase shift between wave height and flap velocity and this justifies the use of a reference velocity signal, since a non-complex (pure-real) control gain can be used.

The actuation signal is composed by two terms. The first one is the flap velocity required to generate the desired wave $v_{dk}$, previously calculated by the generation transfer function (equation 3.1). The second term is responsible for the absorption of reflected waves $v_{ak}$ . In the present work, a third term was also included, in order to avoid drifting of the flap, keeping its motion around the neutral position:

$$v_k = v_{dk} - v_{ak} - K x_k \tag{4.1}$$

In the relation above, $v_k$ is the imposed velocity of the flap, $k$ is the number of the flap, $x_k$ is the flap position with respect to its neutral position and $K$ is an adjustable control gain (used to avoid the drift). The component responsible for the wave absorption was simplified, considering a perpendicular incidence angle:

$$v_{ak} = \frac{2\pi f_p}{F_p} \eta_{rk} \tag{4.2}$$

where $f_p$ is the instantaneous estimated wave frequency, $F_p$ is the progressive transfer function (equal to $c_0$) and $\eta_{rk}$ is the reflected wave elevation.

During the preliminary tests in a 2D wave flume (described in the next section), high-frequency oscillations of the flaps were observed. A possible explanation for such fact is the influence of evanescent modes in the measured wave height, which were neglected during control derivation. A correction was then introduced in the reflected wave elevation measurement (Kawaguchi, 1986), considering that evanescent wave modes and flap acceleration present approximately no phase shift ($K_{acc}\,\partial^2 x_k / \partial t^2$). Furthermore, a reduction in the overall gain of the controller was also included ($K_p$). The final formulation for the reflected wave elevation is then given by:

$$\eta_{rk} = K_p(\eta_k - \eta_{dk}) + K_{acc} \frac{\partial^2 x_k}{\partial t^2} \tag{4.3}$$

where $\eta_k$ is the wave elevation measured in the flap $k$ and $\eta_{dk}$ is the reference wave elevation, previously calculated by equation 3.1.

The instantaneous frequency of reflected wave is obtained from standard frequency estimation algorithms. In the present paper, the following relation was used:

$$f_p = \frac{1}{2\pi} \sqrt{-\frac{1}{\eta_{rk}} \frac{\partial^2 \eta_{rk}}{\partial t^2}} \tag{4.4}$$

## 5 Absorption algorithm B

The second algorithm is based on Schäffer (2001). Similar to the first algorithm, it also uses the free surface elevation in front of each wave maker as hydrodynamic feedback, but here the position reference is used as control signal.

This algorithm is developed in time domain and includes the effects of the evanescent modes. Considering a perpendicular incidence angle, the wavemaker position $X_0$ can be formulated as:

$$X_0 = (2A_I - A_0) F_0 \tag{5.1}$$

$$F_0 = \frac{1}{i \sum_{j=o}^{\infty} c_j^*} \tag{5.2}$$

where '*' denotes complex conjugate. $A_I$ is the complex amplitude of incident wave $\eta_{dk}$, $F_0$ is a complex transfer function

related to the inverse of the flap generation transfer function ($A_0/X_0$) and its implementation in time domain is made by a recursive digital filter:

$$\tilde{F} = \frac{\sum_{k=0}^{M_1} a_k z^{-k}}{1-\sum_{k=1}^{N_1} b_k z^{-k}} \tag{5.3}$$

The coefficients $a_k$ and $b_k$ can be obtained by optimization to match $\tilde{F}$ and $F_0$, remembering that the poles of the digital filter must be within the unit circle in the z-plane to guarantee stability. During the optimization, high frequency responses should also be forced down to avoid instability, as shown, for example, in Figure 2.

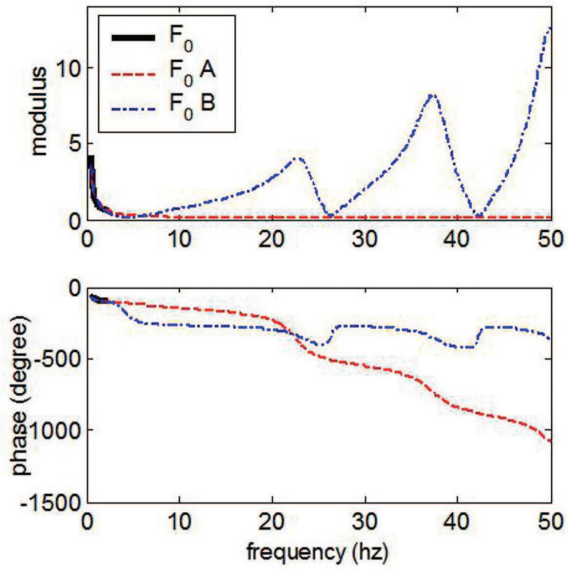


(a) Full frequency range

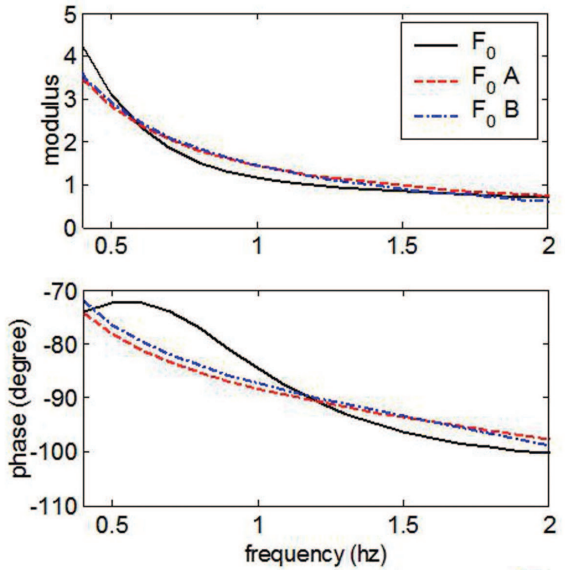


(b) Desired frequency range

Fig. 2 Example of filter optimization , where $F_0$ is the target filter, $F_0A$ was optimized considering high frequency response and $F_0B$ was optimized using only the desired frequency range.

The delay originated from the position loop motor control can be compensated by optimizing $F_{0M} = F_{0/M}$ instead of the original absorption transfer function $F_0$. The final block diagram of the absorption control system is showed in Figure 3.

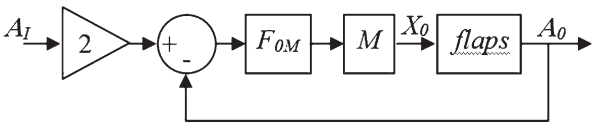


Fig. 3 Diagram of the control absorption algorithm B.

## 6 Experimental setup

Both absorption algorithms were tested in a wave flume at the Naval Arch. & Ocean Eng. Dept. at Escola Politécnica. The wave flume is 25m long, 1.0m wide, the still water level is 0.8m and it is equipped with an edge type wave maker.

To absorb the waves, a prototype wave generator composed of four independent flaps (Figure 4) was installed on the opposite side of the original wave maker. Each flap is equipped with an ultrasonic wave sensor mounted on its face, based on the propagation time of pulse-echo, as described by Martins et al. (2007).

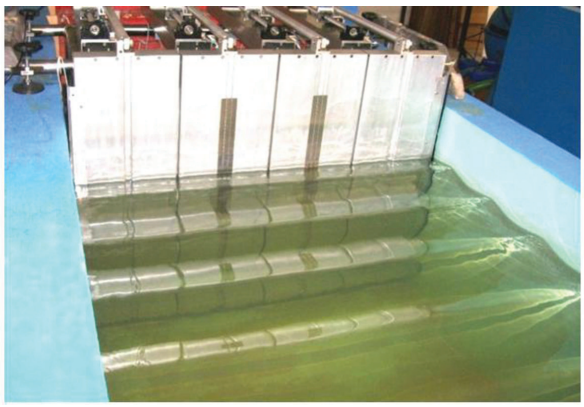

Fig. 4 Prototype absorbing wavemaker.

The experiments consisted of testing the absorption of regular waves with different amplitudes and frequencies generated by the original wave making system. The reflection coefficient ($Cr = A_r/A_I$) was estimated by the method proposed by Mansard & Funke (Isaacson, 1991) and implemented by de Mello (2006), using the signals gathered by an array of wave probes installed in the center of the wave flume, as shown in Figure 5.

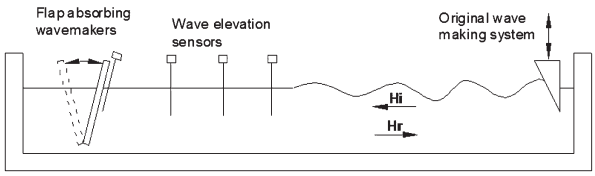


Fig. 5 Experimental setup

## 7 Results

In the present section, the results obtained with the absorption algorithm in the wave flume are presented and discussed. Figure 6A shows an example of wave elevation measured by the wave probe installed on the absorbing flaps when they are inactive. The progressive wave height generated by the original wave-maker system is approximately 15 mm. It can be seen that, due to the reflection in the inactive flaps, the elevation is almost doubled as soon as it reaches the flap (during the first 50s), since the sensor measures the sum of incident and the reflected waves. After that interval, the reflected waves reached the wave-making system, reflected on it, and returned to the flaps. This second reflection occurred in approximately 50~60s, and can be clearly noticed in the figure.

When the flaps are active, on the other hand, the absorption algorithm avoids the reflection of a major part of the incident wave. Figure 6B shows the replication of the previous experiment, now with the flaps operating. The efficiency of the method can be readily noticed. In this case, the wave amplitude remains approximately constant around 15~17mm.

In order to optimize the control parameters of the absorption algorithm A, a trial and error fine-tuning procedure was used for each case to obtain the smallest reflection coefficient. Only the best result is presented for each generated wave.

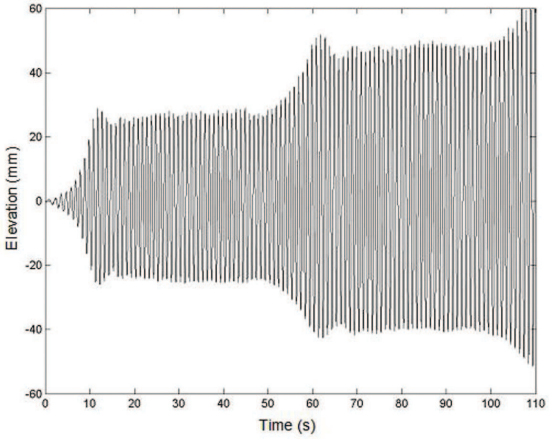


(a) Absorption inactive

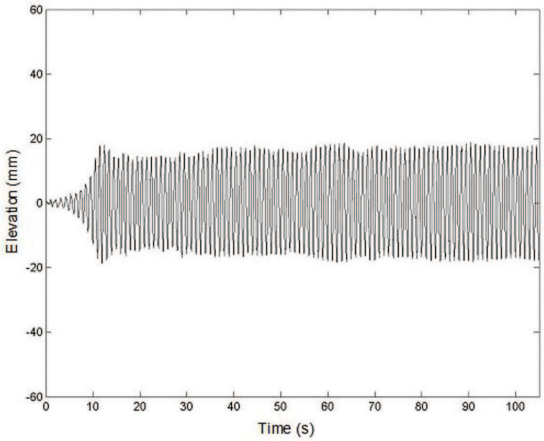


(b) Absorption active

Fig. 6 Example of generated waves.

Figure 7 presents an example of the time series of the reflection coefficient Cr, incident and reflected wave heights estimated for the two different absorption algorithms. This test corresponds to a wave frequency of 1.0 Hz. The average reflection coefficient during the interval between 80s and 140s is 6.7% for algorithm A and 7.9% for algorithm B.

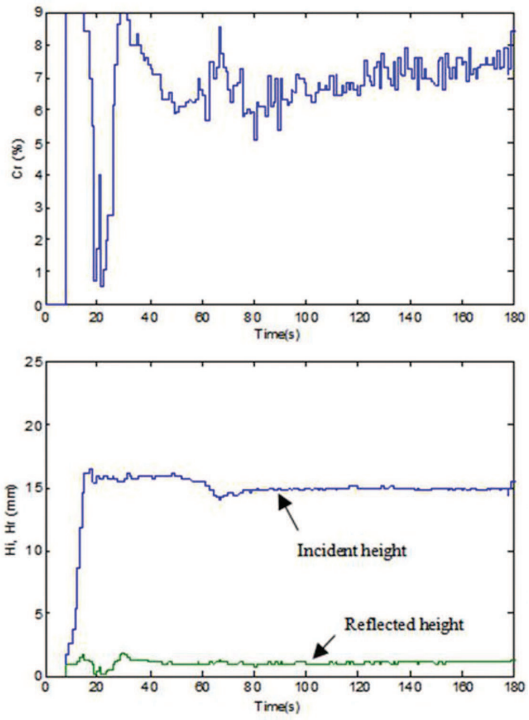


(a) Algorithm A

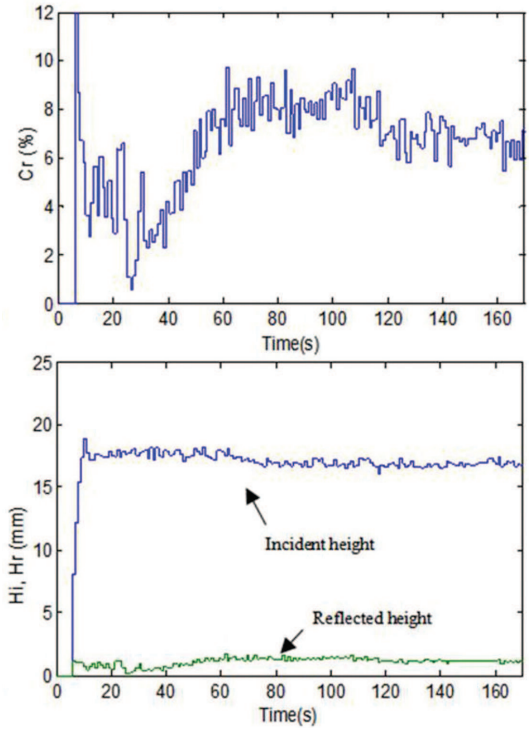


(b) Algorithm B

Fig. 7 Example of experimental reflection coefficient (1.0 Hz wave).

In order to absorb irregular waves, estimation of the instantaneous wave frequency $f_p$ is necessary at each time step. This estimation is applied to correct the control parameters $K$, $K_p$ and $K_{acc}$. During the tests with regular waves, however, it was observed that the frequency estimation by means of equation 4.4 is very sensible to level sensor noise. A long averaging mean filter with period of 1.0s was required to obtain a reasonable result, consequently delaying the frequency estimation response. Figure 8 shows an example of the estimated frequency before and after the filtering and the correspondent elevation time series for a regular wave of frequency 1.0 Hz.

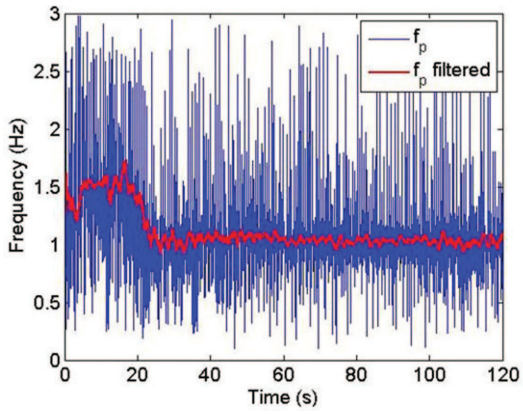


(a) Frequency estimation

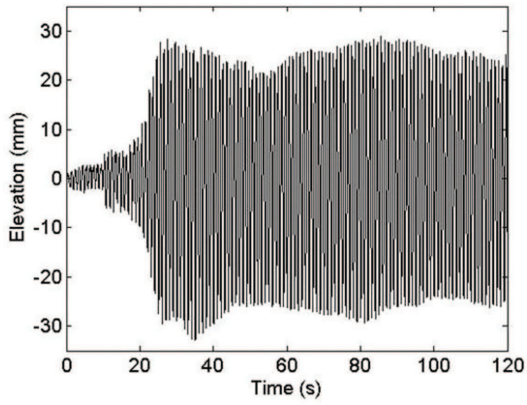


(b) Elevation time series

Fig. 8 Example of frequency estimation.

Table 2 shows a summary of the results for the absorption algorithm A. It can be seen that the reflection coefficient was smaller than 11% for all cases tested, what is considered quite acceptable. Control parameters adjusted for each case are also presented.

**Table 2** Summary of experimental results – Absorption algorithm A

| Frequency (Hz) | Height (mm) | Kp | Kacc | K | Cr (%) |
|---|---|---|---|---|---|
| **0.50** | 12 | 0.64 | -0.0074 | 0.14 | 10.7 |
| **0.75** | 18 | 0.69 | -0.0077 | 0.14 | 3.4 |
| **1.00** | 15 | 0.76 | -0.0085 | 0.14 | 6.7 |
| **1.00** | 20 | 0.76 | -0.0085 | 0.14 | 5.3 |
| **1.50** | 16 | 0.53 | -0.0047 | 0.14 | 10.6 |

During the tests with the absorption algorithm B, high frequency oscillations were also observed, than a reduction in the overall gain of the controller was also included (Kp). This is the only parameter to be adjusted. The summary results can be seen in Table 3:

**Table 3** Summary of experimental results – Absorption algorithm B

| Frequency (Hz) | Height (mm) | Kp | Cr (%) |
|---|---|---|---|
| **0.50** | 25 | 0.67 | 10.3 |
| **0.75** | 25 | 0.67 | 7.2 |
| **1.00** | 18 | 0.80 | 7.9 |
| **1.50** | 15 | 0.80 | 10.1 |

## 8 Conclusions

In the present paper, a discussion about the wave generation and absorption algorithms to be implemented in the TPN wave basin was presented.

Generation is based on the time realization of the frequency domain transfer functions of each flap, considering their linear superposition. Generation algorithms for regular and irregular waves, with or without directional spreading, were studied, but experimental validation still needs to be conducted.

Two different absorption algorithms were tested using a small scale prototype in a 2D wave flume. Results indicated that:

- Both algorithms presented acceptable performance for regular waves, with reflection coefficients smaller than 11% for wave frequencies between 0.5Hz and 1.5Hz.
- Algorithm A requires a time-consuming tuning process, in order to adjust at least two control parameters. For each wave frequency, a new tuning procedure is required.
- Algorithm A is executed in frequency domain and an online algorithm for wave frequency estimation is also required when considering irregular waves.
- Algorithm B has only one tuning parameter (control gain *Kp*), that is theoretically equal to 1. A reduction in this control gain was introduced in order to avoid high frequency oscillations.
- Algorithm B is executed in time domain, and no frequency estimation is required.
- Convergence, stability and tuning of the frequency estimation algorithm are yet to be evaluated, and may pose another drawback concerning the application of Algorithm A.

Based on the considerations above, algorithm B, which was based on the original method proposed by Schäffer (2001), was chosen for the control system to be implemented on the TPN wave basin.

## Acknowledgments

The authors acknowledge Petrobras for the financial support and for the motivation of this work. The first author acknowledges the São Paulo State Research Foundation (FAPESP Proc. No. 2008/06428-4). Fifth and sixth authors also acknowledge the Brazilian National Research Council (CNPq) for the research grants.

## References

Dean, R. G., and Dalrymple, R. A. (1984), "Water wave mechanics for engineers and scientists", Prentice-Hall, Inc., Englewood Cliffs, New Jersey.

Isaacson, M. (1991), "Measurement of regular wave reflection," Journal of Waterway, Port, Coastal, and Ocean Engineering, Vol. 117, No. 6, pp. 553-569.

Kawaguchi, T. (1986), "Absorbing wave making system with wave sensor and velocity control," Mitsui Zosen Technical review, No. 128, pp. 20-24, (in Japanese).

Maeda, K., Hosotani, N., Tamura, K., and Ando, H. (2004), "Wave making properties of circular basin", International Symposium on Underwater Technology, pp. 349-354.

Martins, J. A. de A., de Mello, P. C., Carneiro, M. L., Souza, C. A. G. F., and Adamowski, J. C.(2007), "Laboratory wave probes dynamic performance evaluation", Proceedings of XX COPINAVAL - Congresso PanAmericano de Engenharia Naval e Transportes Marítimos, São Paulo, Brazil.

de Mello, P. C. (2006), "Reduction of reflected waves in wave tank with parabolic beach", M.Sc. Dissertation, COPPE, Federal University of Rio de Janeiro, Rio de Janeiro. Available at: http://www.oceanica.ufrj.br/intranet/modules/rmdp/down. php?id=35 (in Portuguese).

de Mello, P. C., Carneiro, M. L., Tannuri E. A., Nishimoto K. (2009), "USP active absorption wave basin: from the conception to the commissioning", 4rd International Workshop on Applied Offshore Hydrodynamics, Rio de Janeiro, Brazil.

Naito, S., Nakamura, T., Sakashita, H., and Tomita, K. (1996), "A new configuration of wave basin and a control of wave generation and absorption-the case when an advancing ship comes across the given waves", Proceedings of the 4th Pacific/Asia Offshore Mechanics Symposium, Vol. 226, pp. 207-212.

Naito, S. (2006), "Wave generation and absorption in wave basins: theory and application", Proceedings 16th International Offshore and Polar Engineering Conference, San Francisco, California, USA.

Nohara, B. T.; Yamamoto, I.; Matsuura, M. (1996), "The organized motion control of multi-directional wave maker", Proceedings of the 4th International Workshop on Advanced Motion Control, v. 2, p. 470-475.

Ochi, M. (1998), "Ocean waves. The stochastic approach", Cambridge Ocean Tech. Series 6, Cambridge Univ. Press.

Salter, S. H.(1981), "Absorbing wave-makers and wide tanks", Proceedings Directional Wave Spectra Applications, Berkeley.

Schäffer, H. A. (1996), "Second-order wavemaker theory for irregular waves", Ocean Engineering, Vol. 23, No. 1, pp. 47-88.

Schäffer, H. A., 2001, "Active wave absorption in flumes and 3D basins", Waves'01: Proc 4th Int. Symp. on Ocean Wave Measurement and Analysis, San Francisco, USA, ASCE, pp. 1200-1208.